

University of Mississippi

eGrove

Honors Theses


Honors College (Sally McDonnell Barksdale
Honors College)

Spring 5-9-2020

Study of Pharmaceutical Tablets Using Raman Mapping

Kyle Joseph Pauly
University of Mississippi

Follow this and additional works at: https://egrove.olemiss.edu/hon_thesis

 Part of the [Complex Mixtures Commons](#), [Medicinal Chemistry and Pharmaceutics Commons](#), [Pharmaceutical Preparations Commons](#), and the [Physical Chemistry Commons](#)

Recommended Citation

Pauly, Kyle Joseph, "Study of Pharmaceutical Tablets Using Raman Mapping" (2020). *Honors Theses*. 1441.

https://egrove.olemiss.edu/hon_thesis/1441

This Undergraduate Thesis is brought to you for free and open access by the Honors College (Sally McDonnell Barksdale Honors College) at eGrove. It has been accepted for inclusion in Honors Theses by an authorized administrator of eGrove. For more information, please contact egrove@olemiss.edu.

Study of Pharmaceutical Tablets Using Raman Mapping

By: Kyle Pauly

A thesis submitted to the faculty of The University of Mississippi in partial fulfillment of
the requirements of the Sally McDonnell Barksdale Honors College.

Oxford, MS

May 2020

Approved by:

Dr. Nathan Hammer
Advisor

Dr. Gerald Rowland
Reader

Dr. Gergory Tschumper
Reader

©2020
Kyle Joseph Pauly
ALL RIGHTS RESERVED

Acknowledgements

Firstly, I would like to thank the University of Mississippi and the Sally McDonnell Barksdale Honors college for giving me a home and a place to grow for the last four years of my life. I would also like to thank Dr. Hammer for mentoring me and pushing me to become a better student and researcher. I am honored to have been a member of The Hammer Lab as they accepted me with open arms and were there to help me whenever possible. Specifically, I would like to thank Genevieve Verville, Austin Dorris, and April Hardin for being my mentors not only in lab but in life. However, none of this would have been possible without the support of my friends, my parents, Quinn and Anne, and my siblings, Ryan, Sean and Farryn.

Study of Pharmaceutical Tablets Using Raman Mapping

Kyle Pauly (under the direction of Dr. Nathan Hammer)

Covalent bonds are the strongest type of bonds holding molecules together. Based on the pattern of bonding of the molecule, the atoms associated with the bond will vibrate at a specific frequency. Utilizing vibrational spectroscopy, such as Raman spectroscopy, these unique vibrational frequencies can be used to detect the presence of analytes over a selected area. Furthermore, the intensities of the vibrational modes can be tracked to comparatively quantify the concentration of analytes at various locations. This is a method of great importance due to its ability to compare pharmaceutical tablets synthesized with different techniques. Here, the presence and concentration of ibuprofen in lipid matrix was observed. This was done in collaboration with a pharmaceutical lab with the hopes of producing a higher quality suppository tablet.

Table of Contents

Copyrights Page	ii
Acknowledgements	iii
Abstract	iv
List of Figures	vii
List of Abbreviations	viii
Chapter 1: Pharmaceuticals	1
1.1 History of Pharmaceuticals	1
1.2 The Drug Development Process	2
1.3 Ibuprofen	4
1.4 Suppositories	5
Chapter 2: Raman Spectroscopy	7
2.1 What is Spectroscopy	7
2.2 Raman Spectroscopy	10
2.3 Principles of Raman Spectroscopy	10
2.4 Applications of Raman Spectroscopy	14
2.5 Instrumentation of Raman Spectroscopy	14
Chapter 3: Raman Mapping	19
3.1 Principles of Raman Mapping	19
3.2 Applications of Raman Mapping	20
3.3 Raman Mapping of Pharmaceuticals	21

Chapter 4: Method Development.....	23
4.1 Calibration and Sample Preparation.....	23
4.2 Reference Spectra	24
4.3 Step Size and Area Mapped.....	26
4.4 Limitations and Errors of Instrument.....	35
Chapter 5: Conclusions and Future Work.....	39
References	40

List of Figures

1. Line structure of the S(+) enantiomer of Ibuprofen	5
2. Electromagnetic Spectrum	8
3. Quantum Mechanically Allowed Transitions	9
4. Scattering Patterns of Raman Spectroscopy	12
5. IR and Raman Active Modes of CO ₂	13
6. Fluorescence versus Stokes Scattering	16
7. Reference Raman Spectra of Ibuprofen and the Lipid Matrix	24
8. Reference Raman Spectra between 1400cm ⁻¹ and 1650cm ⁻¹	25
9. Composition of Spectra Gathered from 5-micron 12,100μm ² Raman Map	27
10. 12,100μm ² Raman map of Ibuprofen with a 5-micron Resolution	28
11. 12,100μm ² Raman map of the Lipid Matrix with a 5-micron Resolution	29
12. 12,100μm ² Raman map of Ibuprofen with a 2-micron Resolution	31
13. Composition of Spectra Gathered from 2-micron 12,100μm ² Raman Map	32
14. 360,000μm ² Raman Map of Ibuprofen with outlined 12,100μm ² Raman Map	34
15. Composition of Spectra Displaying Baseline Error	35
16. Composition of Spectra Gathered from 25,000,000μm ² area	36
17. 25,000,000μm ² Raman Map of Ibuprofen with 25-micron Resolution	37

List of Abbreviations

FDA	Food and Drug Administration
NSAID	Non-Steroidal Anti-Inflammatory Drug
COX-1	Cyclooxygenase-1
COX-2	Cyclooxygenase-2
UK	United Kingdom
EMS	Electromagnetic Spectrum
UV	Ultraviolet
IR	Infrared
YAG	Yttrium Aluminum Garnet
CCD	Charged Coupled Device
API	Active Pharmaceutical Ingredient
SEM-EDX	Scanning Electron Microscopy combined with Energy-Dispersive X-Ray Spectroscopy
XRPD	X-Ray Powder Diffraction
TAT	Transactivator of Transcription
MCF	Michigan Cancer Foundation
COVID-19	Coronavirus Disease of 2019

Chapter 1: Pharmaceuticals

1.1 History of Pharmaceuticals

A pharmaceutical is described as a substance that is used for the diagnosis, treatment, or prevention of a disease. This substance usually evokes beneficial response that results in the restoration, correction, or modification of organ functions. This process has existed for centuries, dating back to ancient civilization consuming medicinal plants and minerals; however, the pharmaceutical revolution began in the 16th century with the construction of the first pharmacopoeia in Germany detailing a list of drugs and their preparation. This resulted in the rapid development of the pharmaceutical industry and has led to modern pharmaceutical approach.¹

At the heart of modern pharmaceuticals in the United States is the Food and Drug Administration (FDA). This federal government agency was established in 1906 as a result of the Federal Food and Drugs Act. In addition, this act outlawed the mislabeling and selling of tainted food, drinks and drugs. This along with the Shirley Act passed in 1911, which outlawed medication from making false medical claims, were the first steps taken by the United States in order to make the pharmaceutical industry more scientific field.² Through trial and error and legislation, the FDA has slowly evolved into its modern form and, as a result, a five-step drug development process is required for every new medication.

1.2 The Drug Development Process

As outlined by the FDA, the drug discovery process consists of five steps: discovery and development, preclinical research, clinical research, FDA review, and FDA post-market safety monitoring.

The discovery and development step begins at the research level. As organ systems and disease become more understood, more molecules are tested to find possible beneficial effects. Thousands of chemicals are tested, but very few make it to later stages of testing. After this initial testing, the chemical properties of the molecules must be further studied to understand how it is absorbed, distributed, metabolized and excreted. This understanding helps researchers and manufacturers to determine the dosage and best method of administration. After this, the compound then moves to the preclinical research stage of development.³

In this stage, in-vitro, test tube and culture tests, and in-vivo, live animal tests, are performed. Since the toxicity of the compounds are discovered in this step, the in-vivo test is typically preformed on animals.⁴ The choice of animal is dependent upon the organ system of interest and ethicality of the experiment. For example, larger animals, such as dogs, cats, and non-human primates, are commonly used as models for cardiology, endocrinology, bone, and joint research. However, a majority of these tests are performed on mice and rats.⁵ The goal of this stage of research is to provide more detailed insight into the dosing and toxicity levels of the compounds before moving into human testing.⁴

The clinic research stage is typically the most important stage of drug development process as it is the first stage in which the drugs are tested on humans. Within this stage of research, there is typically three to four phases of human research. These tests begin

small in size, 20-100 people, to confirm the safety and dosage of the drug. After this, the tests get larger in size and begin to focus in on the efficacy and side effects of the drugs. The time period of these tests range from a few months to up to four years. If the drug has evidence of effectiveness and is seemingly safe, the drug developer files an application to the FDA to market the drug.⁶

This application must include the proposed labeling, safety, dosing, and directions of use. In addition, all of the studies, data, and analysis have to be shared with the FDA. Once this application has been completed, the review team analyzes the sections of application based on the specialties of the individual reviewer. For example, a pharmacologist will review the data from animal studies. As well as reviewing the application, the laboratory is also inspected for any signs of fabrication, or withheld data. The review team has six to ten months to make a decision on whether or not to approve the drug. After this total review, the review team offers a recommendation to a senior FDA official who makes the final decision regarding the marketing of the proposed drug.⁷

Once a drug hits the market, the FDA continues to monitor its safety and efficacy. The FDA also monitors advertisement to ensure the information provided is truthful and sufficiently describes the side effects. This is a continuing process that lasts the entire length of product's lifetime in the marketplace. Lastly, when the initial patents of the drugs expire, generic brands can be made following the original instructions, and do not require the manufacturers to undergo as rigorous of testing since this was already done when the initial patent was filed for.⁸

In this thesis, the stage of development that was concentrated on was discovery and development. The collaborator to this experiment provided samples mixed in various ways

with a novel instrument to be analyzed using Raman mapping. The goal of this was to provide experimental data to ensure the proper mixing and an even distribution of the active ingredient. Once the method was established, the goal was to then analyze a sample with more active ingredients.

1.3 Ibuprofen

The initial active ingredient analyzed was ibuprofen. This drug is a propionic acid derivative that was introduced in 1969 as an alternative to aspirin. Today, it has become the most commonly used and prescribed non-steroidal anti-inflammatory drug (NSAID). Its function is to inhibit cyclooxygenase-1 (COX-1) and cyclooxygenase-2 (COX-2), which are enzymes involved in the synthesis of prostaglandins. These prostaglandins are lipid autacoids that play a key role in the inflammatory response.⁹ Inflammation is a response by the immune system to infection and injury. Typically, inflammation is a healthy and beneficial response as it leads to the removal of offending factors and restores tissue and physiological function. However, these prostaglandins also play an important role in the production of pain and, therefore, are a key target for pain reducing drugs.¹⁰ In addition, due to its single chiral center, there exists two enantiomers: R(-) and S(+). The S(+) enantiomer inhibits the cyclooxygenases, whereas the R(-) enantiomer becomes involved in the lipid metabolism pathway and is incorporated into triglycerides. Interestingly, 50-60% of the R(-) undergoes metabolic inversion to the S(+) enantiomer depending on the dosing situations. Therefore, due to the safety and inversion of the enantiomers, ibuprofen is typically taken as a racemic mixture.¹¹ The structure of the S(+) enantiomer of Ibuprofen is shown in **Figure 1**.

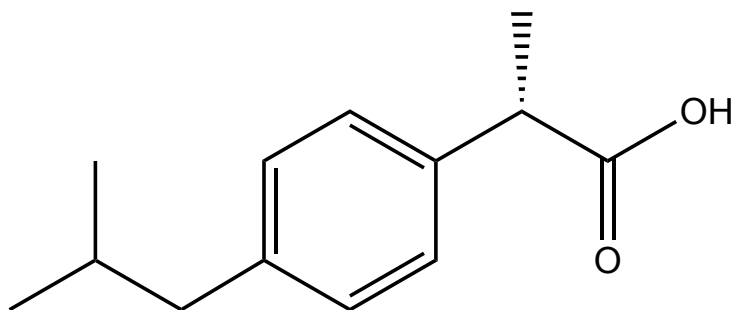


Figure 1. Line structure of the S(+) enantiomer of Ibuprofen.

Ibuprofen is typically taken orally with a potency of 200 to 800 mg. It is available as an over the counter medication and has been rated as the safest conventional NSAID in the UK. It has a maximum daily dose of 3200 mg, with over dosage resulting in seizures, apnea, and hypertension⁹. It has been shown to have therapeutic application for patent ductus arteriosus, rheumatoid and osteo-arthritis, cystic fibrosis, orthostatic hypotension, dental pain, dysmenorrhea, fever, and headaches.⁹

1.4 Suppositories

There are six general routes of entry into the body for drug administration. In order of fastest to slowest central nervous system response, these are: intravenous, inhaling, snorting, oral, and rectal.¹² Suppositories often follow the rectal route of entry. Though its absorption is typically slow, it offers many advantages as well. By avoiding the stomach, acidic and enzymatic degradation of the drug can be avoided as well as irritation of the stomach and small intestine. In addition, these medications can be taken before surgeries and by patients with upper gastrointestinal diseases. Furthermore, the delivery of the medication can be stopped in cases of accidental overdose by simply removing the suppository.¹³

Rectal suppositories are typically inserted as a solid, and then are slowly dissolved within the body. The medication is then taken up by the epithelial cells lining the rectum. From here, the medication passes through the lower and middle hemorrhoid veins and enter systemic venous circulation via the internal iliac veins.¹³ Due to this mode of entry, the medication circumvents the liver and, therefore, does not undergo first pass metabolism. This increases its bioavailability.¹³

Chapter 2: Raman Spectroscopy

2.1 What is Spectroscopy?

Spectroscopy is defined as the study of interactions between light and matter. Light is electromagnetic radiation with a consistent speed depending on the medium that it travels through. In addition, light has a characteristic referred to as wave-particle duality. This principle states that light exhibits properties of both waves and particles. This particle is referred to as a photon.¹⁴ An understanding of both of these properties is required for spectroscopy as the energy of this photon of light is determined by its wavelength. This theory which is shown in **Equation 1.1** was proposed by Einstein who postulated that the amount of energy, E , carried by a photon depends on its frequency, ν , multiplied by Planck's constant, h .¹⁴

$$E = h\nu \quad (1.1)$$

Furthermore, frequency is equal to the speed of light, c , divided by its wavelength, λ . This expands **Equation 1.1** into **Equation 1.2**:

$$E = \frac{hc}{\lambda} \quad (1.2)$$

Planck's constant, $6.626 \times 10^{-34} \text{ J}\cdot\text{s}$, and the speed of light, $3.00 \times 10^8 \text{ m/s}$, are both constants. Therefore, there is an inversely proportional relationship between the energy and wavelength of light. The full range of wavelengths and their corresponding energies is shown in **Figure 2**.

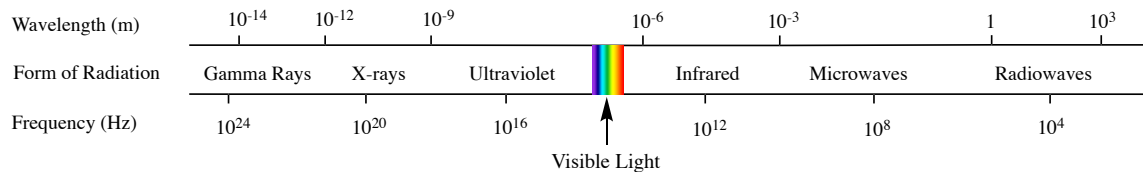


Figure 2. Electromagnetic Spectrum.

At the core of the interaction between light and molecules is the concept that atoms and molecules exist at well-defined energy levels. Quantum chemistry defines four primary energy levels for molecules: electronic, vibrational, rotational, and translational.¹⁵ Due to their lack of bonding, only electronic and translational energy levels exist for atoms. These energy levels can be experimentally analyzed with light due to the fact that a photon can only be absorbed or emitted if its energy is equivalent to the energy gap between two atomic or molecular quantum energy states.¹⁵ Typically, the magnitude of these transitions is as follows: Electronic > Vibrational > Rotational > Translational¹⁵. A schematic depicting these transitions is shown in **Figure 3**. Based on this understanding, different energy level transitions result from different regions of the EMS. For example, Electronic transitions are comparatively large, so high energy light, such as ultraviolet (UV) or visible light, must be used to probe these transitions. On the other hand, lower energy light, such as a microwave, is needed to probe rotational transitions. Therefore, spectroscopic instruments typically utilize specific regions of the EMS to analyze the unique molecular transitions of analytes.¹⁵ For example, IR spectroscopy, as the name suggests, analyzes the absorption of infrared light by a molecule. IR spectroscopy is a form of vibrational spectroscopy and its absorption arises from a net change in dipole moment of a molecule. Dipole moment refers to the magnitude of the charge separation in polar covalent bonds.

Therefore, only asymmetric vibrational modes can be analyzed with this technique as the net charge separation of symmetric vibrational modes is always zero.¹⁵

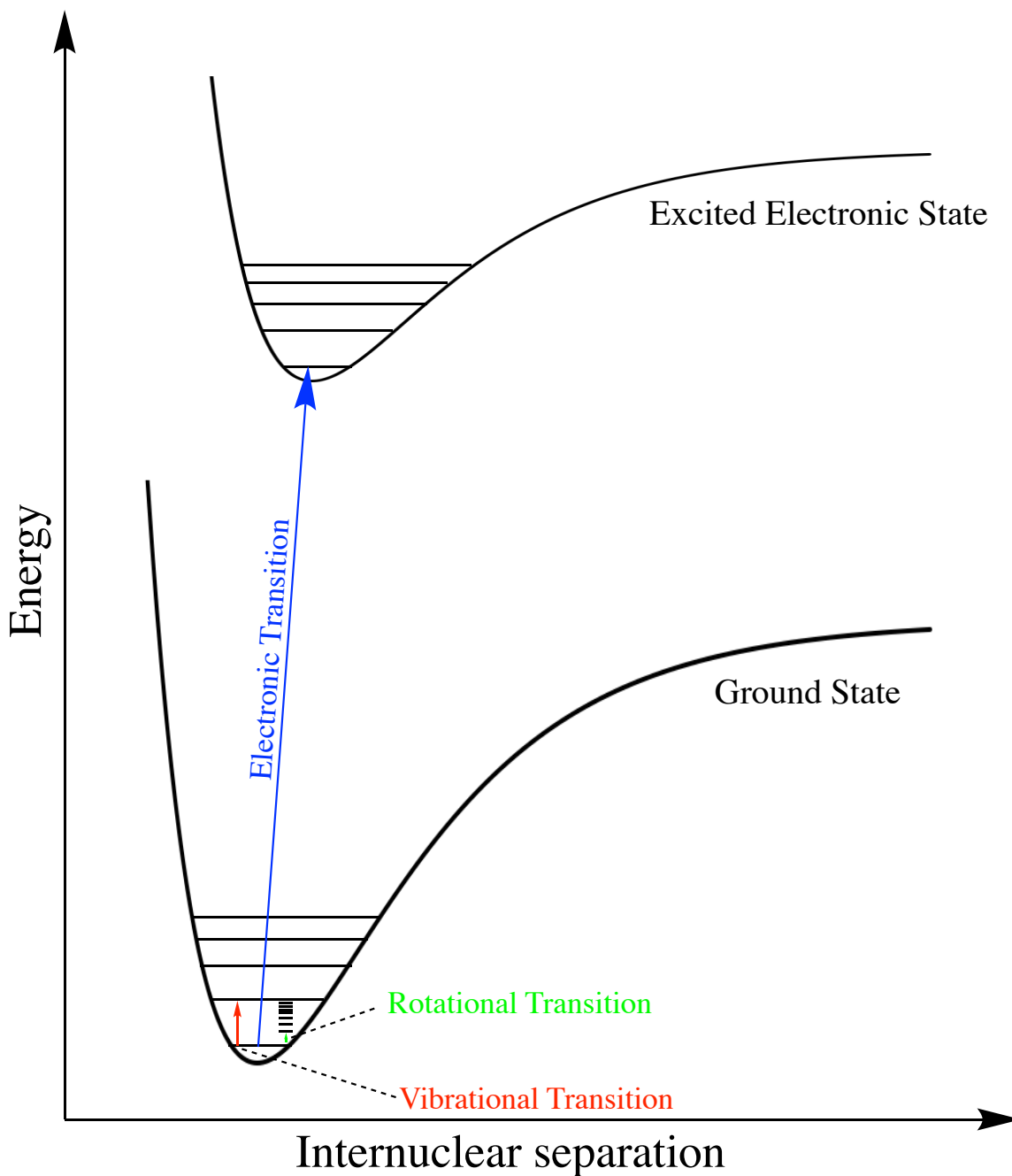


Figure 3. Quantum Mechanical Transitions.

2.2 Raman Spectroscopy

When analyzing benzene with a mercury lamp, Sir C.V. Raman observed an unexpected wavelength in the light scattered from benzene. This became known as the Raman Effect and the unknown spectrum he observed was the Raman spectrum of benzene. As he explored this phenomenon more, he found that, regardless of the excitation wavelength, the change in wavelength was consistent for a given molecule.¹⁵ However, Sir Raman, was not the first person to observe scattering. Previously, Lord Rayleigh had explained that the color of the sky was due to the elastic scattering of light by the molecules in the atmosphere.¹⁶ As a result, the ideas of these great minds combined to form the foundation of Raman spectroscopy.

2.3 Principles of Raman Spectroscopy

Complementary to IR, Raman spectroscopy is also a form of vibrational spectroscopy. Rather than absorption or emission of light, Raman spectroscopy occurs due to the scattering of photons by a molecule. This scattering is best described as an absorption of light by a molecule to excite it to a virtual state, which is nearly immediately followed by the emission of light.¹⁵ As opposed to other forms of spectroscopy, this virtual state can exist at any energy level. Yet, so as to not break any quantum rules, this virtual state exists for around 10^{-13} seconds and is only achievable under strong electromagnetic conditions.¹⁵ These conditions are supplied by the laser. After this virtual state is achieved, the photon will then be emitted by the molecule. There are three possible emission patterns for this photon. The first of these is Rayleigh scattering. If the molecule, originally in a ground state, is excited up to the virtual state and then falls back into the ground state,

Rayleigh scattering has occurred. As previously stated, this is an elastic form of scattering as the incident and emitted light have the same energy. This is not useful for Raman spectroscopy because no molecular properties are revealed.¹⁵ Therefore, the only useful scattering patterns for Raman spectroscopy are inelastic scattering in the forms of Stokes and anti-Stokes scattering. Stokes scattering occurs when the molecule, originally in the ground state, is excited to the virtual state. This time, however, it falls into an excited vibrational state. Therefore, the emitted photon now has less energy as some energy was absorbed by the molecule.¹⁵ Finally, anti-Stokes scattering occurs when the molecule is already in an excited vibrational state. When the molecule emits a photon, the electron returns to the vibrational ground level; this causes the emitted photon to be higher in energy than the incident photon. Anti-Stokes is the rarest form of scattering as it requires the molecule to be in an excited vibrational state before analysis. However, the incidence of anti-stokes scattering can be increased by heating the sample.¹⁵ For research purposes though, only Stokes scattering is typically observed. The Raman scattering patterns are shown in **Figure 4**.

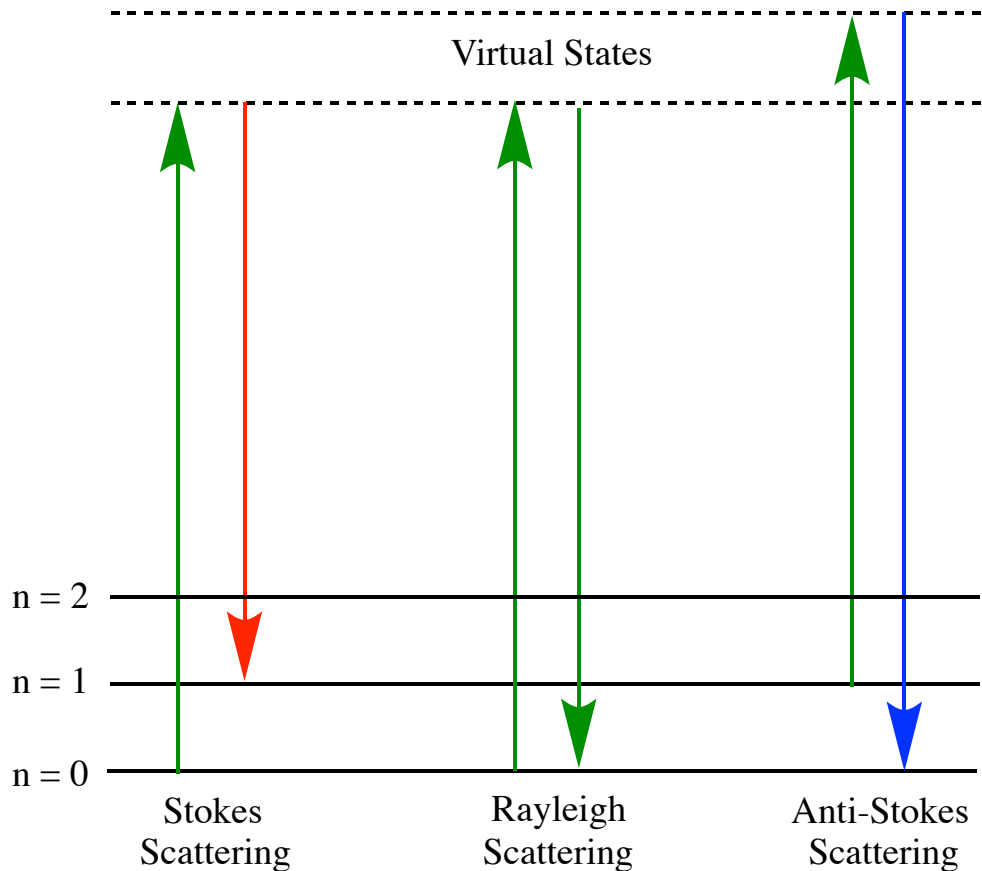


Figure 4. Scattering Patterns of Raman Spectroscopy.

The importance of the inelastic scattering is the difference in energy between the incident, λ_0 , and transmitted light, λ_1 . This is referred to the Raman shift, $\Delta\tilde{\nu}$, and it is what is graphed when analyzing a Raman spectrum.¹⁵ Raman shifts, similarly to IR spectroscopy, are recorded as wavenumbers, cm^{-1} . This observed shift is therefore calculated using

Equation 1.3:

$$\Delta\tilde{\nu} = \left(\frac{1}{\lambda_0 [\text{nm}]} - \frac{1}{\lambda_1 [\text{nm}]} \right) \cdot 10^{-7} \text{ nm cm}^{-1} \quad (1.3)$$

Additionally, not all vibrational modes can be analyzed with Raman spectroscopy. For Raman, a change in polarizability, α , of the molecule is required. Polarizability is defined

as the difficulty of an external electronic field to distort the electron cloud of an atom of molecule.¹⁵ This concept is shown in **Equation 1.4**.

$$\mu_{\text{induced}} = \alpha E \quad (1.4)$$

μ_{induced} is defined as the induced dipole moment and E refers to the external electric field. A change in polarizability is observed during symmetric stretching modes of molecules. This is because the simultaneous stretching and compressing of adjacent bonds significantly changes the electron cloud of a molecule.¹⁵ Antisymmetric modes, other the other hand, will not undergo a change in polarizability because the relative distances between the atoms are all the same. Furthermore, bending modes are also generally Raman inactive. This is because the change in polarizability is symmetric throughout bend, therefore there is no net change in polarizability.¹⁵ Interestingly, vibrational modes that are IR active are typically Raman inactive and vice versa. A common example of this property is the antisymmetric and symmetric stretching modes of CO₂ shown in **Figure 5**.¹⁵

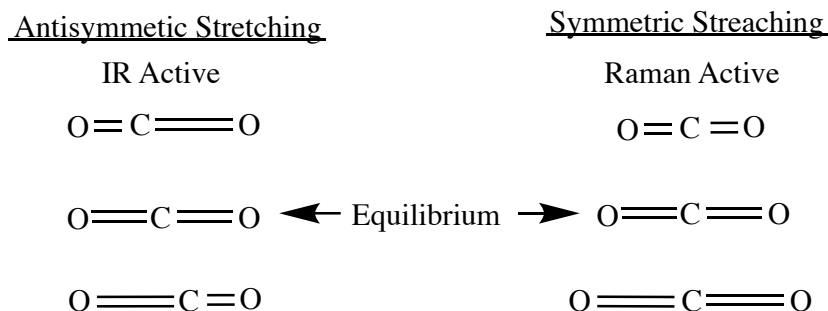


Figure 5. IR and Raman Active Modes of CO₂.

This is why these spectroscopic methods are typically regarded as complementary. However, it is possible for vibrational modes to be both Raman and IR active, or neither. An example of a Raman and IR active vibrational mode is the HF stretching mode. This

is because both the polarizability and dipole moment change as the molecule stretches and compresses. Both these methods, when used in conjunction will provide the best overall understanding of the nature of the vibrational modes in the analyzed molecules.¹⁵

2.4 Applications of Raman Spectroscopy

Raman spectroscopy has become an increasing common analytical technique. Its main application is the identification of organic, inorganic, and biological samples.¹⁵ In fact, most applications where a non-destructive, microscopic, chemical analysis, and/or imaging technique is required can be probed with Raman spectroscopy.¹⁷ This is accomplished by comparing the observed spectral peaks with characteristic group frequencies.¹⁸ From these observed peaks, insights about the molecule's vibrational modes are gathered, as well as its interactions with solvent molecules.^{19,20} In addition, this method can also be used to confirm the presence of molecules in complex mixtures by identifying molecule specific peaks within the obtained spectrum.²¹ Furthermore, this form of spectroscopy is not limited by the phase of the analyte. Solids, liquids, gases, gels, slurries, and powders can all be analyzed with Raman Spectroscopy.¹⁷

2.5 Instrumentation of Raman Spectroscopy

The components of a typical Raman spectrometer include a radiant source, a wavelength discriminator, filters, and the detector. Typically, the radiant light source for Raman spectroscopy is a laser in the visible range of the EMS.¹⁵ The visible region is usually an ideal option of light source for Raman spectroscopy because an optimal Raman light source excites the molecule without inciting electronic absorptions, as this would

result in fluorescence which would overwhelm the Raman signals.¹⁵ The chosen laser should possess sufficient energy such that the virtual state is higher in energy than the vibrational levels of the ground electronic state, allowing for analysis of all possible vibrational states. In order to further show this, a comparison between stokes scattering and fluorescence are shown below in **Figure 6**. Common Raman lasers include argon ion lasers (488 nm or 514 nm), diode lasers (785 nm or 830 nm), Nd:YAG lasers (532 nm or 1064 nm), and neon-copper lasers (248 nm).¹⁵

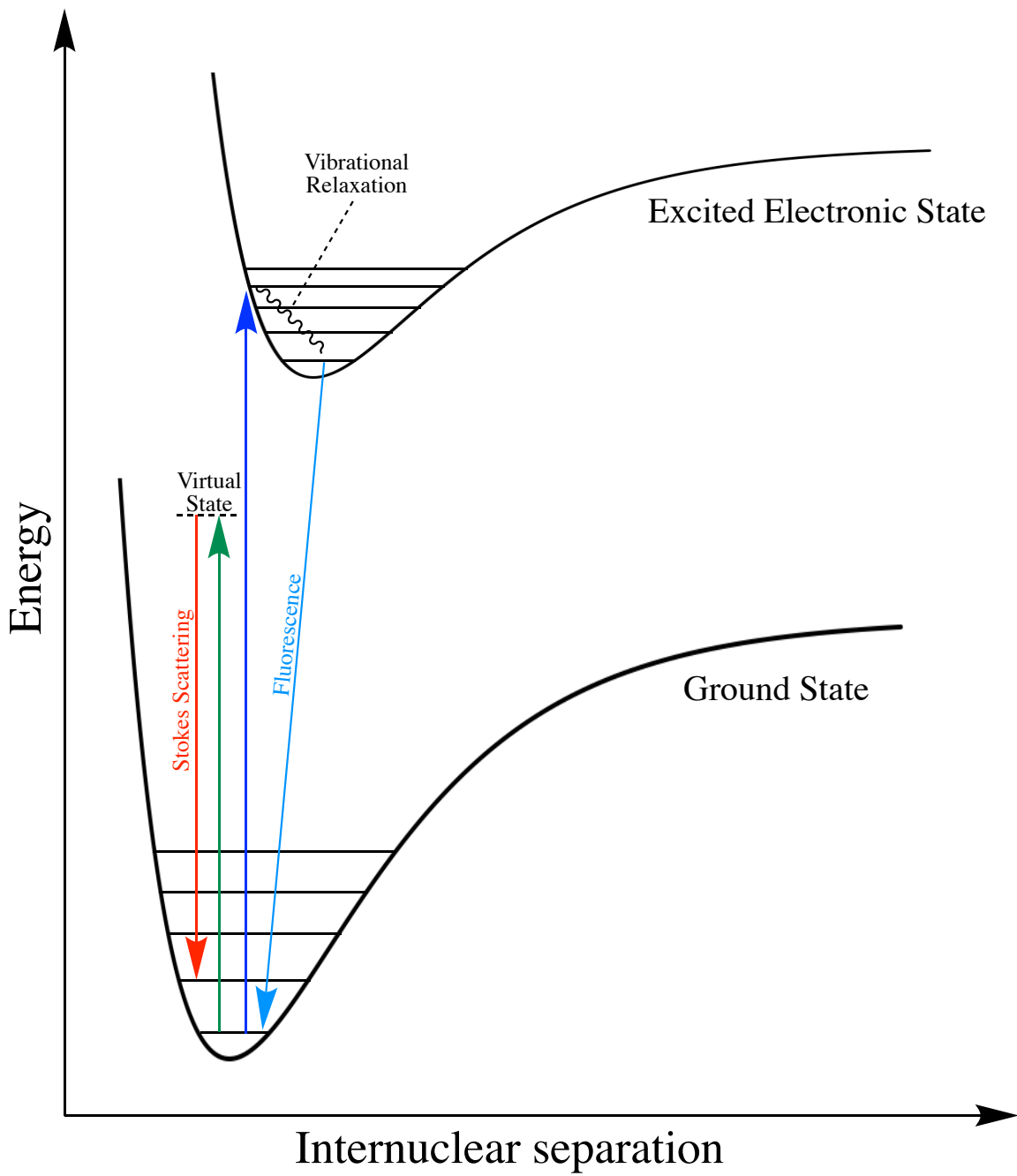


Figure 6. Fluorescence versus Stokes Scattering.

In order to differentiate between the wavelengths of light, diffraction grating is implemented. Essentially, the grating refracts the light at a wavelength dependent angle.¹⁵ However, the light travelling to travel to adjacent gratings will travel different distances to get to their respective grating. Depending on the length of this additional distance traveled, constructive or destructive interference can occur. Constructive interference leads to bright lines being reflective off the grating. Therefore, the goal is to only measure the light reflecting at an angle that produces constructive interference. This angle is determined using the grating equation shown in **Equation 1.5**.

$$\Delta s = m\lambda = d(\sin\alpha + \sin\beta) \quad (1.5)$$

Δs refers to the difference in path length, m is the order of reflection, λ is the wavelength of the incident light, d is the grating spacing, α is the incident angle, β is the angle of the reflected light. An order of zero refers to simple reflection, while higher orders refer to the points of constructive interferences depending on the wavelength of the incident light. Additionally, as higher orders are used, the resolution of the signal improves but the optical signal is reduced and ultimately lowers the signal to noise ratio. When a monochromator is used, first order diffraction is implemented. This includes m values equal to $+1$ and -1 .¹⁵ A given grating's ability to discriminate between wavelengths, λ and $\lambda + \Delta\lambda$, effectively is referred to as its resolving power, R .

$$R = \frac{\lambda}{\lambda + \Delta\lambda} \quad (1.6)$$

This resolving power can be further related to the order, m , and the number of grooves, N , within the grating.

$$R = mN \quad (1.7)$$

In addition to grating, filters are also implemented to block the Rayleigh scattered light while allowing Raman scattered light pass through.¹⁵ Finally, a detector is used to convert the electromagnetic energy of the scattered photons into an electrical energy. The most common detector in modern Raman spectrometers are silicon charge coupled device (CCD) detectors. This detector is sensitive to electromagnetic radiation between ~400 and ~1,000 nm. This detector can be further enhanced through cooling which reduces the thermal noise and, therefore, increases the signal to noise ratio.¹⁵

Additional components can be added to the Raman spectrometer to improve its functionality.

Chapter 3: Raman Mapping

3.1 Principles of Raman Mapping

Raman mapping is a branch of Raman spectroscopy. In fact, in order to perform Raman mapping, the instrumentation remains the same, but a motorized x-y-z stage must be fitted onto the instrument to move the sample from point to point.²² In principle, Raman mapping involves collecting spectral data over a defined area or volume.¹⁹ In addition to Raman mapping, another similar method is referred to as Raman imaging. The function of both of these methods is to analyze spectra over an area, but the difference revolves around sample movement. In Raman mapping, the sample is moved, but in Raman imaging, the area of the CCD is utilized by recording the spectra at each pixel within the detector. Due to the typically large area of the CCD detector, the sample can be analyzed at multiple points simultaneously without sample movement.¹⁹ However, wavelengths of light must be analyzed individually, slowing the process. Here, the process of Raman mapping is expanded upon.

As previously stated, Raman mapping involves the translational motion of the sample. As the sample moves from point to point, a point source is used to capture the Raman spectra at each location.^{19,22,23} From here, two common approaches can be implemented to analyze the Raman maps: univariate and multivariate. In the univariate approach, reference samples of the individual constituents are analyzed and spectral-specific bands that are free of interferences from other constituents are used to classify the analytes within the system.^{19,24,25,26} These bands are then further characterized by their position, area, or height. In comparison, multivariate methods do not require prior spectral

information and improves interpretation of results. Within this method, each component receives a score or parameter, which is mapped at each location analyzed.^{19,22} This score or parameter is based on the agreement to theoretical or reference spectra and the intensity of the peak.^{19,25,27}

3.2 Applications of Raman Mapping

Regardless of the method of analysis, the goal is typically to produce a composite image illustrating the distribution of all of the components within the analyzed area.¹⁹ By classifying molecule specific peaks, the presence of the analytes can be determined at the various points in the mapped area. In addition to these qualitative studies, quantitative studies can also be performed with this technique. The rarity of Raman scattering plays a key role in this as increasing the concentration of analyte increases the chances of Raman scattering occurring if all other experimental parameters are held constant.^{15,19,28} Furthermore, if calibrated with reference material of known concentrations, a calibration curve can be created to determine the concentration of analyte throughout the analyzed area.²⁸ However, without a calibration curve, the intensities can still be used to comparatively quantize the concentrations of analyte within the system if experimental parameters are consistent.¹⁹

In addition to producing composite images, Raman mapping can also be used to gather spectroscopic information about a system over a larger area. To ensure a comprehensive spectrum is obtained, individual Raman spectra can be collected at various spatial locations, as would be done for a composite image, and then averaged.²⁹ This method becomes useful when analyzing large analytes such as protein. For example,

this strategy was used to observe the aggregation of α -synuclein amyloids, which are present in large amounts within Lewy bodies. These Lewy bodies are a diagnostic hallmark of Parkinson's disease, so understanding their formation is of great importance.²⁹

3.3 Raman Mapping of Pharmaceuticals

The most common use of Raman mapping within the pharmaceutical industry is to track the distribution of the active pharmaceutical ingredient (API) for their density and blending distribution pattern. Multiple components can be tracked simultaneously with this technique. Understanding the distribution of API in tablets is of particular interest because the drug release rate is primarily determined by the distribution of the drug.¹⁹ In addition, from the Raman maps, the particle size and spatial distribution of the API can be estimated leading to consistent production of products.²⁷ This is important because it can give insights about the manufacturing process and can then lead to optimization. In fact, Raman Mapping can be implemented at each step of the manufacturing process to monitor and check for induced transitions and then check for drug stability to determine shelf life.²⁶ An example of this is an experiment in which Raman mapping was implemented to characterize the API and cyclodextrin formulations. This is important as cyclodextrins improve the dissociation characteristics of drugs. 0.8mm^2 to 1mm^2 maps were produced with step sizes of $40\mu\text{m}$. Three peaks that were specific to the API at 1581cm^{-1} , 1586cm^{-1} , and 1372cm^{-1} were determined to be markers for the API. Therefore, changes in these peaks would indicate formation of an API-cyclodextrin formation. Six different forms of cyclodextrins were analyzed and the formation of the API-cyclodextrin were analyzed over the mapped area. This data was then compared to the results obtained via scanning electron

microscopy combined with energy-dispersive X-ray Spectroscopy (SEM-EDX) and X-ray powder diffraction (XRPD). The results showed that Raman mapping is an effective to characterize the API-cyclodextrin formation over the analyzed area.³⁰

Raman maps can be taken at different points of the drug dissolution process. This can give provide information about the physical changes that occur during the drug release progress and ensure a consistent release of the API.³¹ In addition to analyzing tablets, Raman mapping has also been employed to observe cellular uptake.^{19,32} This was accomplished by tracking the uptake of unmodified and TAT peptide modified liposome into human breast carcinoma MCF-7 cells over 24 hours. To ensure proper detection, both of the analyzed liposomes were deuterated in order to distinguish them within the cells.³²

As will be discussed further, the limitations of Raman mapping arise due to the time required to collect data. Typically, areas analyzed with Raman range from $25\mu\text{m}^2$ to $\sim 10\text{mm}^2$.¹⁹ However, as the area analyzed gets larger, the time of acquisition increases as well. As instrumentation improves, it will open the door to new applications and make it an even more powerful technique.

Chapter 4: Method Development

In this experiment, the goal was to analyze the distribution of API within a suppository tablet using Raman mapping. However, due to this being a relatively novel technique to the laboratory, the entire method of analysis needed to be constructed. The underlying issues that were initially confronted were: the classification of the ingredients, the time taken to analyze, the area of analysis, and the construction of a 3D representation of the whole suppository. In order to better define the method, a suppository containing just two ingredients, ibuprofen and a lipid matrix, was analyzed. Understanding this, reference spectra of pure samples of the individual analytes were gathered. From this, spectral-specific bands could be selected to monitor the analytes. Additional testing could then be performed to further optimize the time and area of analysis.

4.1 Calibration and Sample Preparation

In order to ensure consistent and precise measurements, the Raman spectrometer was calibrated before collecting any data. This was done by obtaining the Raman shift for a silicon wafer. Crystalline Silicon has a distinct peak at 520 cm^{-1} relative to the laser line, so aligning the detector with this known value establishes that the data produced by the instrument is accurate.³³ In terms of sample preparation, it was previously established that Raman requires little to no sample preparation. However, due to the large shape of the suppository, cross sections had to be collected by slicing the suppository with a utility blade which had proved successful in a previous experiment.³⁴ Care was taken to have the cross sections be as flat as possible so avoid the laser coming out of focus which can lead to signal fluctuations.²⁷

4.2 Reference Spectra

A univariate approach was applied to this experiment. Therefore, spectral-specific peaks with good clarity and separation were needed for each of the analyzed molecules. To accomplish this, reference spectra of pure ibuprofen and the lipid matrix were obtained as shown in **Figure 7**. The 532nm Nd:YAG laser with 100x objective, 100% laser power, and a 600 gr/mm grating with a 10 second acquisition time for 3 acquisitions was employed to record these reference spectra.

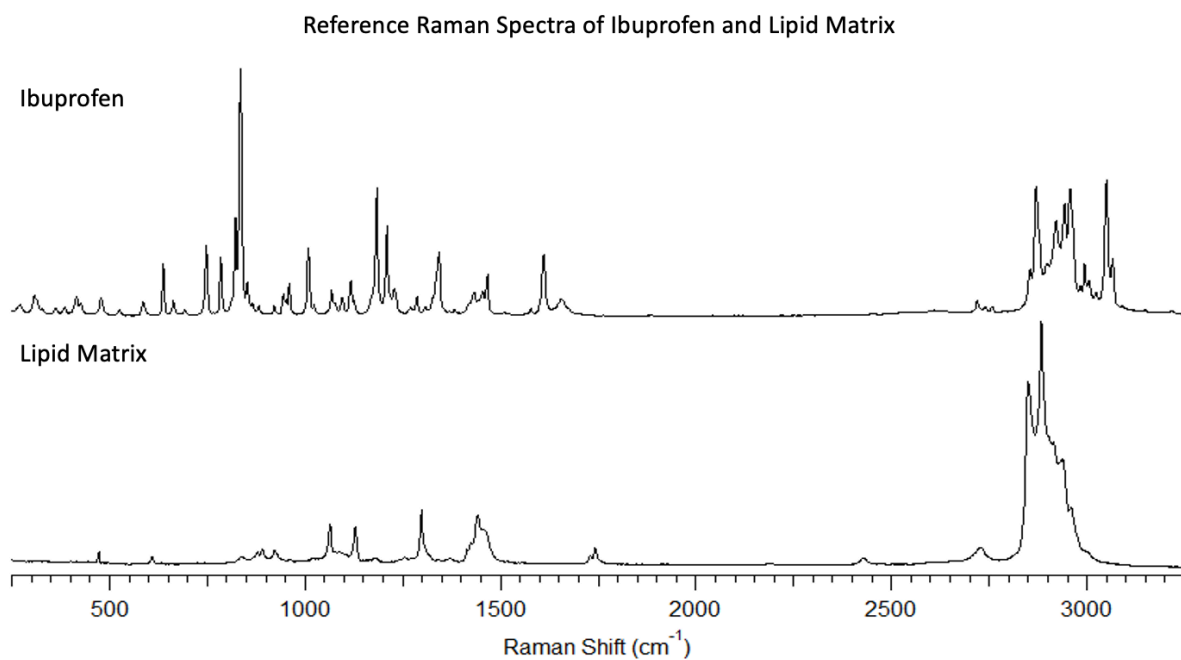


Figure 7. Reference Raman Spectra of Ibuprofen and the Lipid Matrix.

When analyzing the reference spectra, a distinct peak for Ibuprofen can be seen at 1610cm^{-1} . This likely represents a C=C stretching mode.³⁵ In addition, the lipid matrix contains unique vibrational modes from $\sim 1410\text{cm}^{-1}$ to 1490cm^{-1} . This likely correlates to CH_2 and CH_3 bending modes.³⁵ Ibuprofen also contains vibrational modes within this region, but the peak at 1442cm^{-1} is significantly more intense as was easily observed in samples containing both the ibuprofen and the lipid matrix. Therefore, it was hypothesized that the presence of both of these analytes could be tracked within the region of 1400cm^{-1} and 1650cm^{-1} as has been done in similar experiments.³⁶ This region and the analyte specific modes are shown below in **Figure 8**.

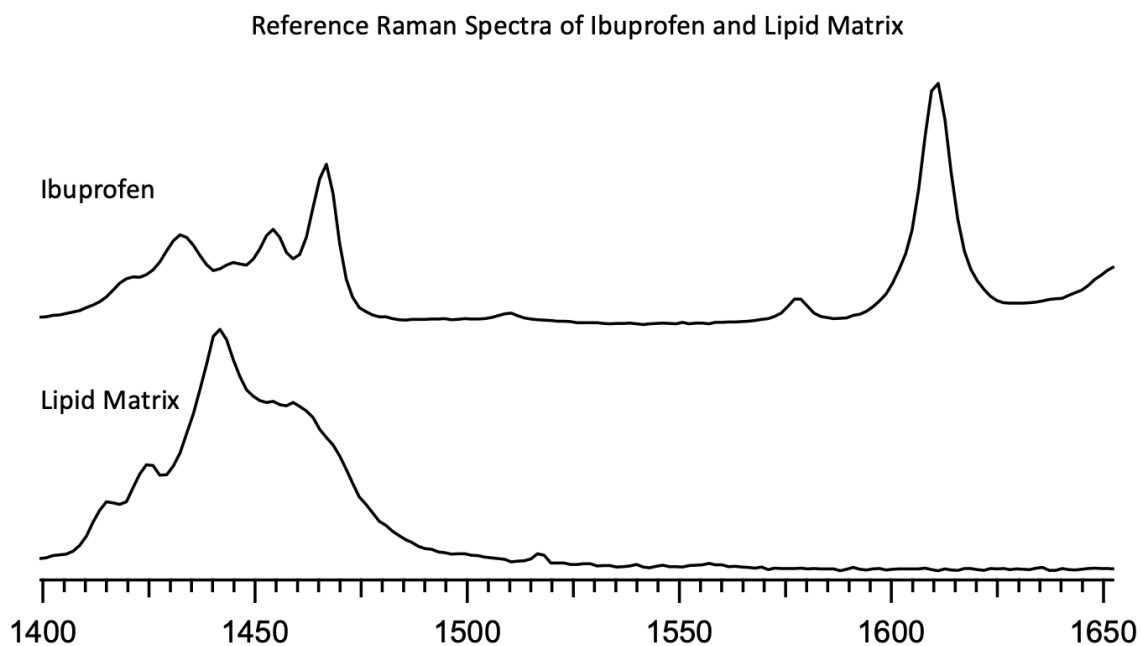


Figure 8. Reference Raman Spectra between 1400cm^{-1} and 1650cm^{-1} .

In addition to the univariate approach, a multivariate approach was also implemented. However, with the multivariate approach, small deviations in peak position

from the reference peaks lead to drastic changes in the outputted intensities displayed within the composite images produced. Using the univariate approach, the peak heights over a small range of wavenumbers could be analyzed allowing for these small deviations to be analyzed without skewing the results, producing more precise results.

4.3 Step Size and Area Mapped

As mentioned earlier, a Raman map is obtained by gathering the spectral data over a defined area. Over this area, the translational stage moves to allow the sample to be analyzed uniformly with a specified distance between the points. The distance between these points is important due to the particle size of the analytes. If the step size is significantly larger than the particle size, the distribution of analytes will not be represented correctly as the laser spot is typically around $1\mu\text{m}$.^{2,21,24,34} Furthermore, the smaller the step size, the longer it will take to analyze the area²¹. Therefore, initially a $110\mu\text{m}^2$ area with a step size of $5\mu\text{m}$ was analyzed. This was performed with the 532 Nd:YAG laser, 100% power, and a 600gr/mm grating with an acquisition time of 3 seconds for 2 acquisitions at each analyzed point. The EMS region of 1400cm^{-1} to 1650cm^{-1} was used. A compilation of all of the spectra gathered during analysis is shown below in **Figure 9**.

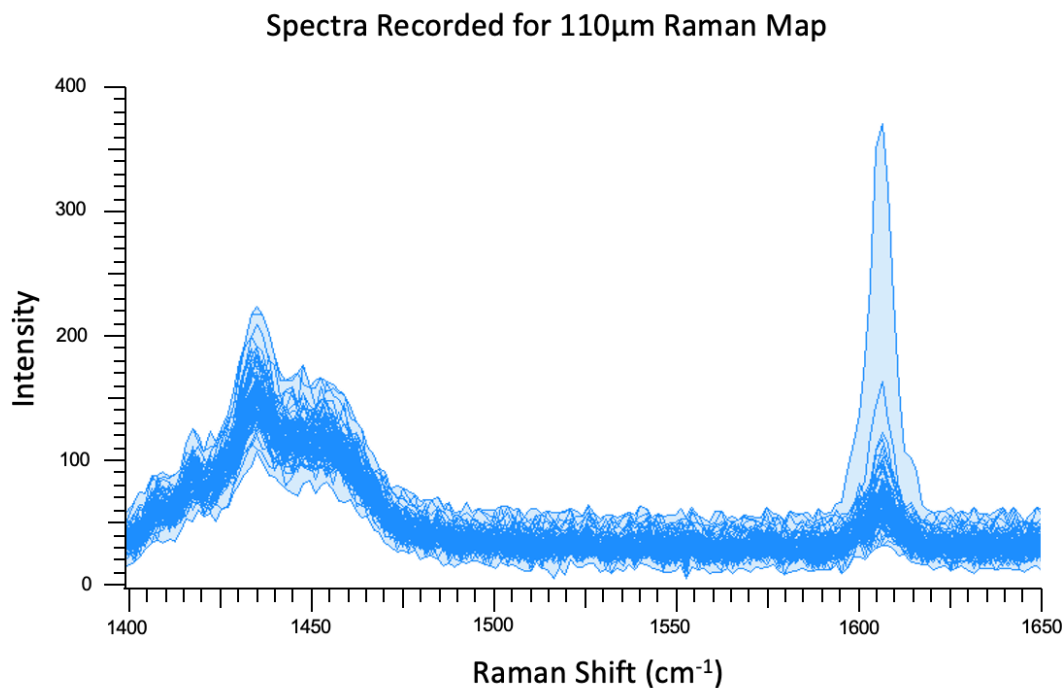


Figure 9. Composition of Spectra Gathered from 5-micron 12,100 μm^2 Raman Map.

From these spectra, the peak at $\sim 1610\text{cm}^{-1}$ can be clearly seen as well as the broad peaks for the lipid matrix from 1410cm^{-1} to 1470cm^{-1} . There is less clarity to these peaks due to the relatively short time and number of acquisitions. However, this quickened time is necessary as these spectra were gathered over the course of six hours. Small increases in these parameters result in significantly more time being required to perform these analyses. Still, the distribution of ibuprofen and lipid can be determined with this method. As these spectra were gathered at distinct locations over the mapped area, it was possible to produce the Raman maps. Using the univariate technique, **Figure 10** and **Figure 11** were produced from this data.

Raman Mapping of Ibuprofen in a Suppository Tablet
5 Micron x 5 Micron Resolution

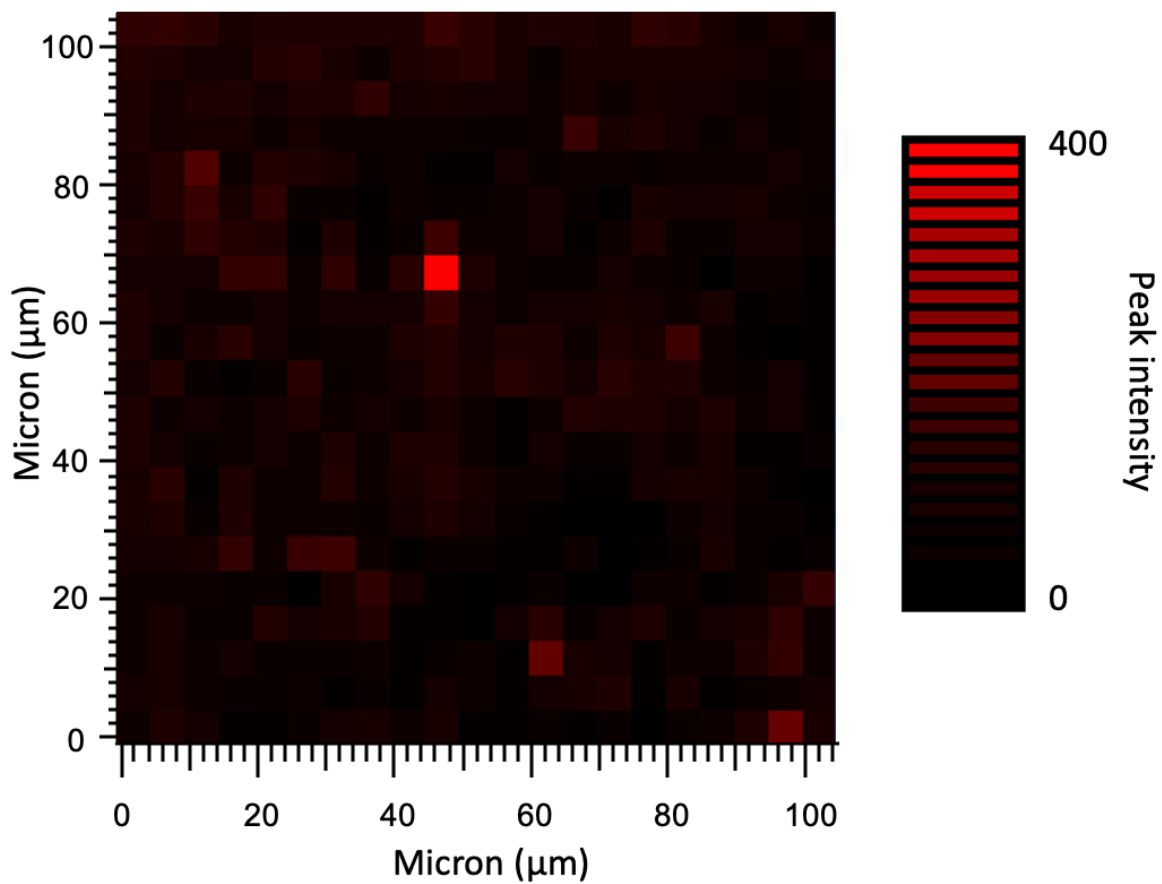


Figure 10. 12,100 μm^2 Raman map of Ibuprofen with a 5-micron Resolution.

Raman Mapping of Fat in a Suppository Tablet
5 Micron x 5 Micron Resolution

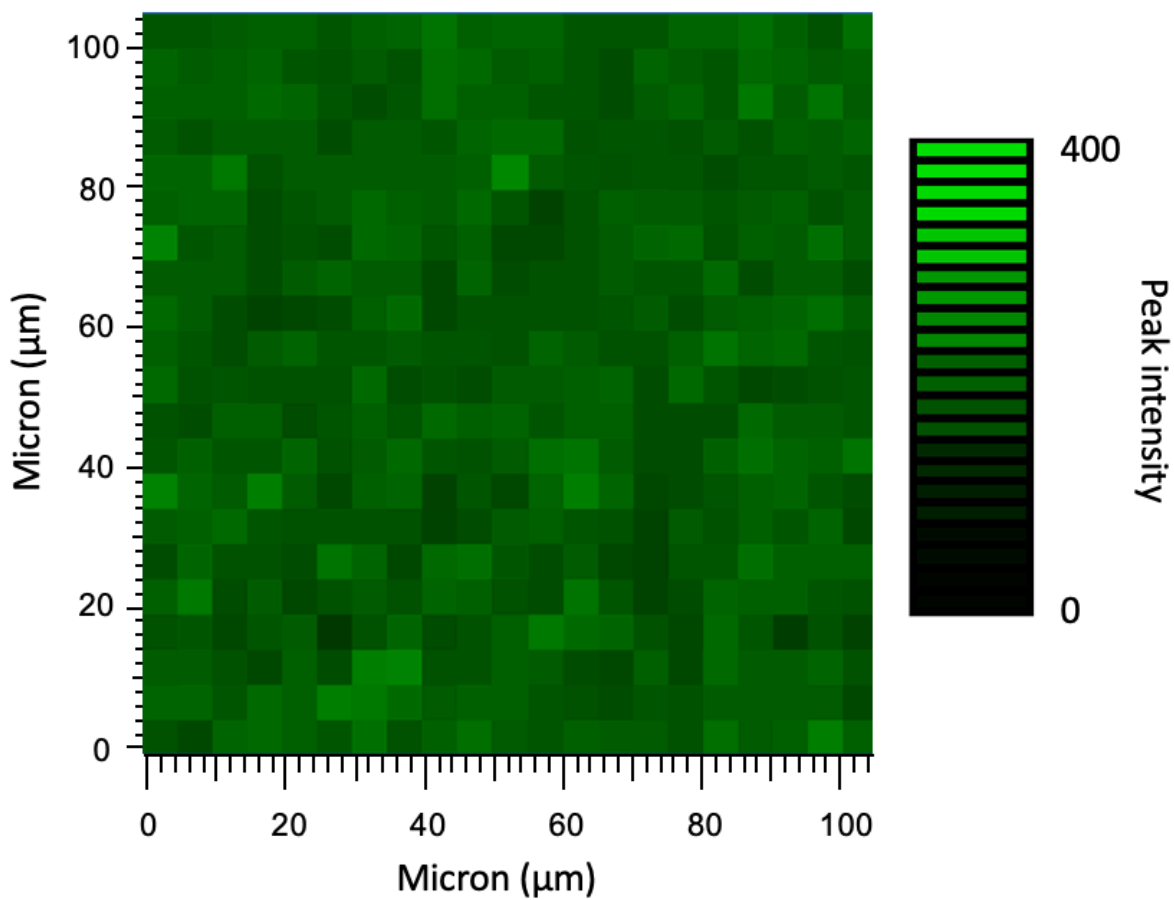


Figure 11. 12,100 μm^2 Raman map of the Lipid Matrix with a 5-micron Resolution.

Within the ibuprofen image, a bright red square can be seen in the center of the image. This correlates to the very intense peak at $\sim 1610\text{cm}^{-1}$ seen in **Figure 9**. This further indicates that a high concentration of ibuprofen is present at this location. However, this also presents as drawback of this method. Due to this point being significantly more intense, the significance of the rest of the points is underestimated. There could be a substantial amount of analyte at other locations that is now being treated as a miniscule in comparison to this point.

Information about the suppository is also revealed from the lipid Raman map. Within the region designating the lipid matrix, peaks were consistently seen with intensities between 150 and 220 counts, signifying a near homogenous distribution of the lipid within the matrix. Based on this assumption, further testing was conducted over a shorter wavelength range in an effort to make a more efficient test.

To confirm the results of this test, another test was performed on this same region of the suppository, but a $2\mu\text{m}$ step size was utilized. All other parameters were held constant. The spectra and composite image are shown in **Figure 12** and **Figure 13**, respectively. From the figures, a very similar distribution of analyte is seen, as well as the intense peak seen towards the center of the gathered image. This supports the conclusion that the distribution was properly captured at the lower resolution. In addition, the spectra for this $2\mu\text{m}$ image were taken over the course of 17 hours further supporting the necessity for a more efficient method.

Raman Mapping of Ibuprofen in a Suppository Tablet
2 Micron x 2 Micron Resolution

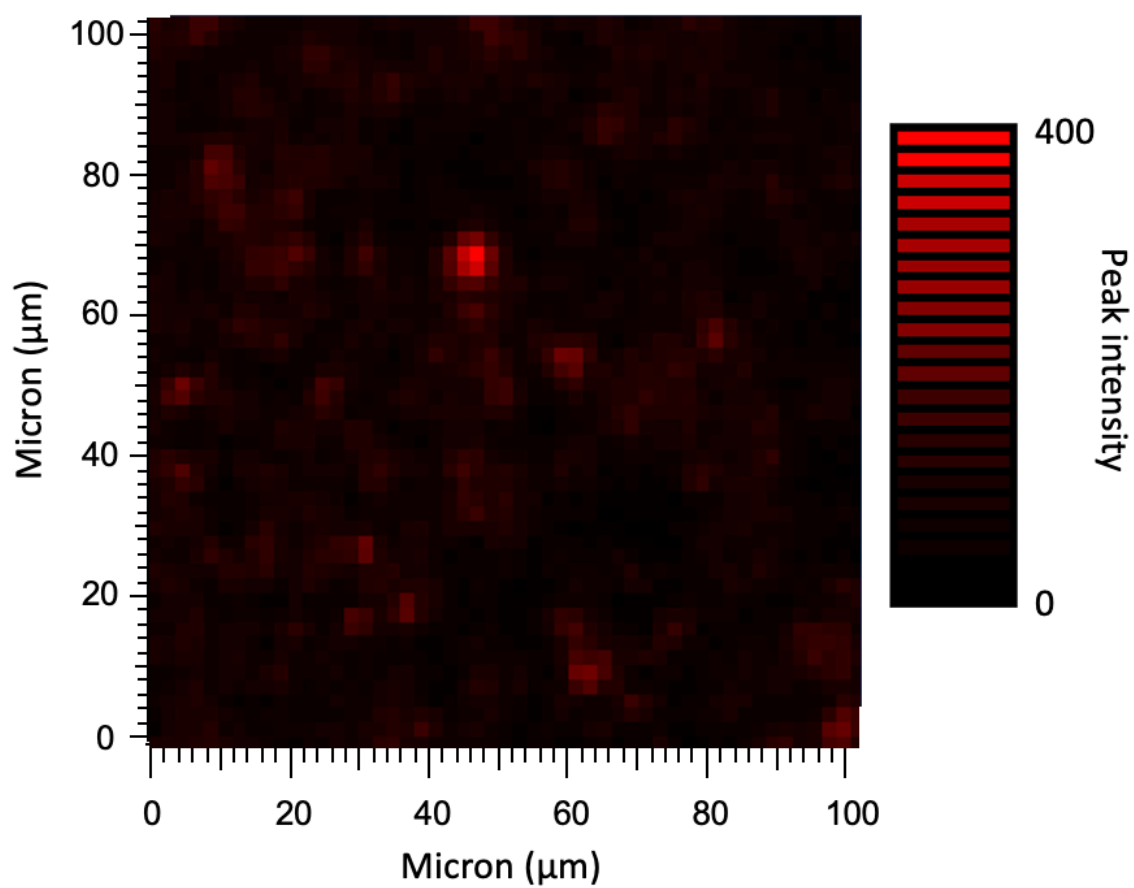


Figure 12. 12,100 μm^2 Raman map of Ibuprofen with a 2-micron Resolution.

All the Spectra Recorded for the 2 Micron Resolution Ibuprofen Map

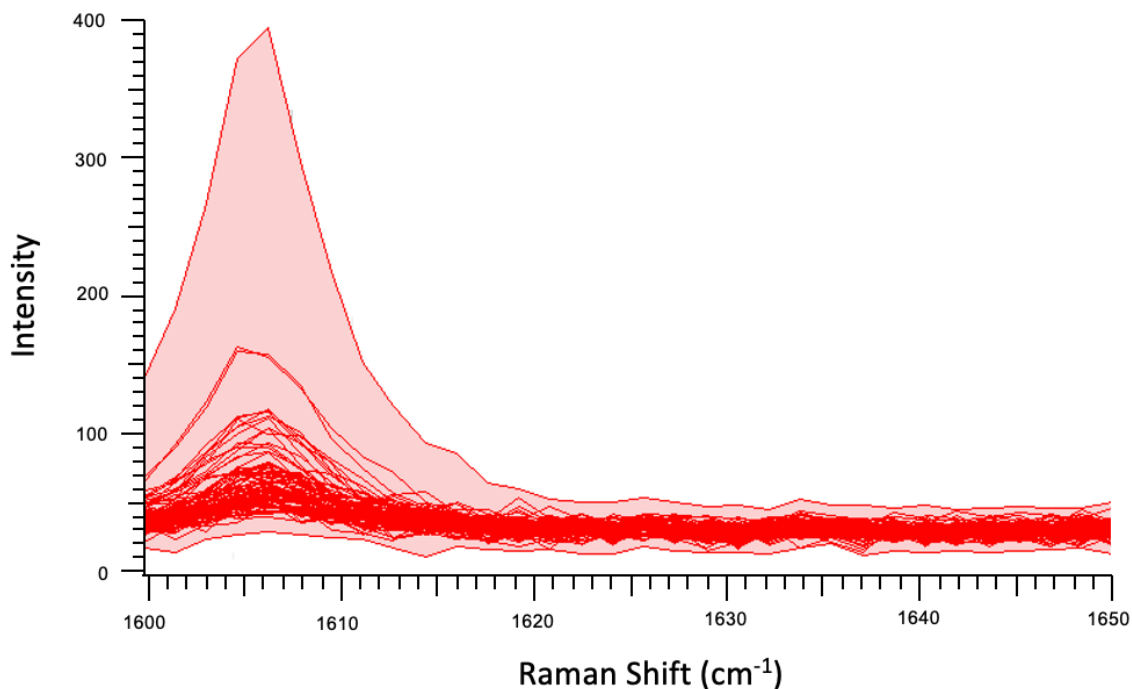


Figure 13. Composition of Spectra Gathered from 2-micron 12,100 μm^2 Raman Map.

Unfortunately, a 12,100 μm^2 area reveals very little about the overall distribution of Ibuprofen in a suppository. The average width of a suppository is roughly half an inch, meaning each cross section would be roughly 1.267 $\times 10^8\mu\text{m}^2$. Therefore, the size of the map also had to be increased. In the next test, a 360,000 μm^2 with a larger step size of 10 μm was analyzed over the wavelength region of 1600 cm^{-1} to 1650 cm^{-1} . One again this was performed with the 532 Nd:YAG laser, 100% power, and a 600gr/mm grating with an acquisition time of 3 second for 2 acquisitions at each analyzed point over the wavelength range of 1600 cm^{-1} to 1650 cm^{-1} . This was also captured in the area around the initially

analyzed $12,100\mu\text{m}^2$ area to determine if the original distribution could be seen within the larger map.

This map is shown below in **Figure 14** along with an outline containing the original $12,100\mu\text{m}^2$ area.

Looking at the outlined area within the composite image, the distribution of ibuprofen was still be reliably captured. Thus, it can be assumed that the distribution was correctly measured throughout the entire scan. Therefore, these were the parameters that were used to conduct further testing.

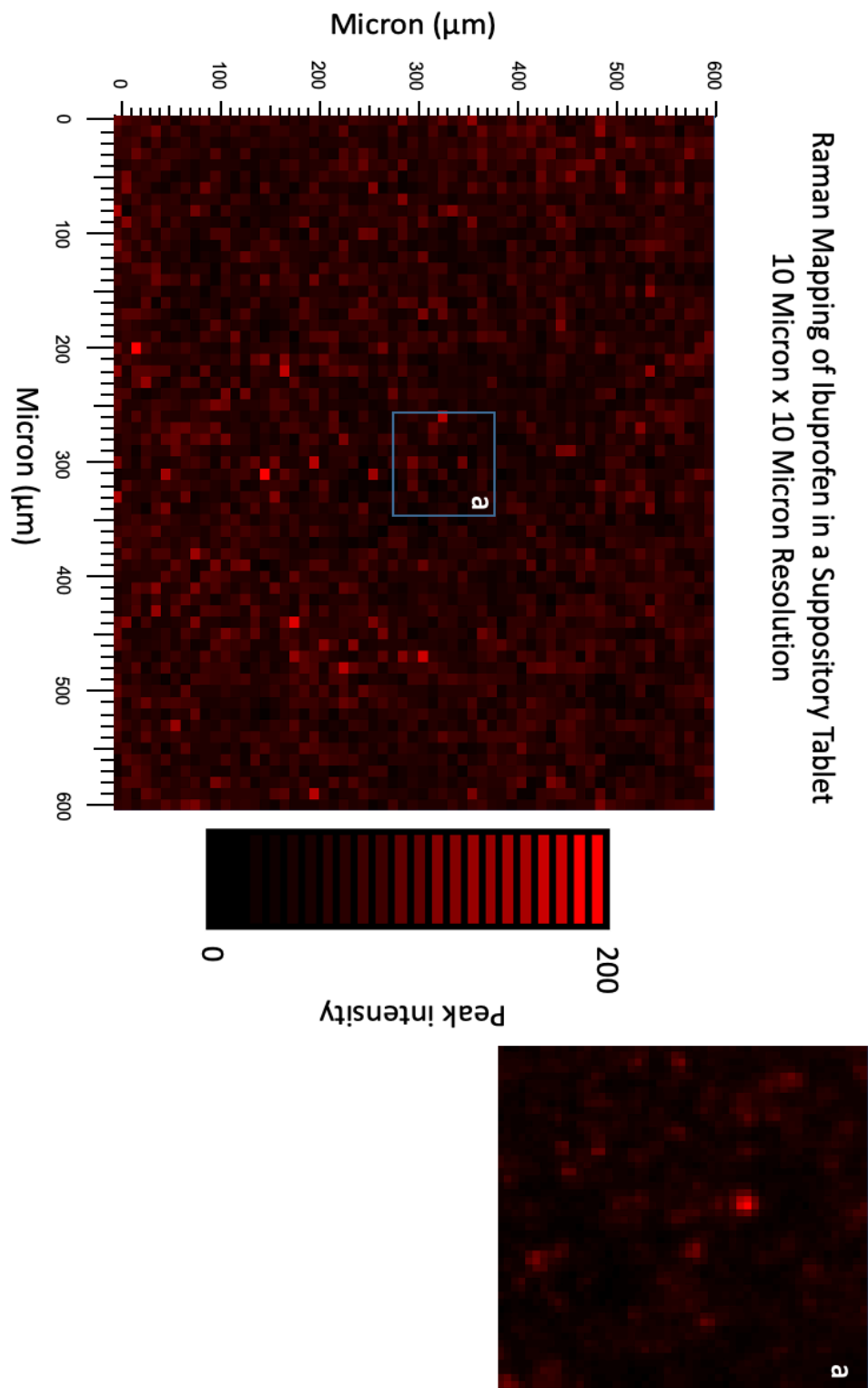


Figure 14. 360,000 μm^2 Raman Map of Ibuprofen with outlined 12,100 μm^2 Raman Map.

4.4 Limitation and Errors of Instrument

It was around this time, that the laser began experiencing issues. The first of these issues pertained to the baseline intensity. As can be seen in **Figure 9** and **Figure 13**, the baseline intensity stays relatively constant. However, spectra like the ones seen in **Figure 15** were soon regularly produced. The cause of this error was unknown, but it led to baseline intensities that varied from 100 to 500 counts. This was a significant issue due to the method of analysis implemented. Using the univariate method of data analysis, the peak height is of great importance, but, with this error, a small signal may be greatly intensified solely based on the intensity of the baseline leading to very inaccurate results. To account for this, a baseline correction was applied to each of the gathered spectra. Interestingly, this also led to curvature within the baseline, producing broad peaks within the region of 1525cm^{-1} and 1575cm^{-1} . Luckily, the peaks around 1610cm^{-1} and 1435cm^{-1} for Ibuprofen and the lipid matrix are still reliably seen. This is shown in **Figure 16**.

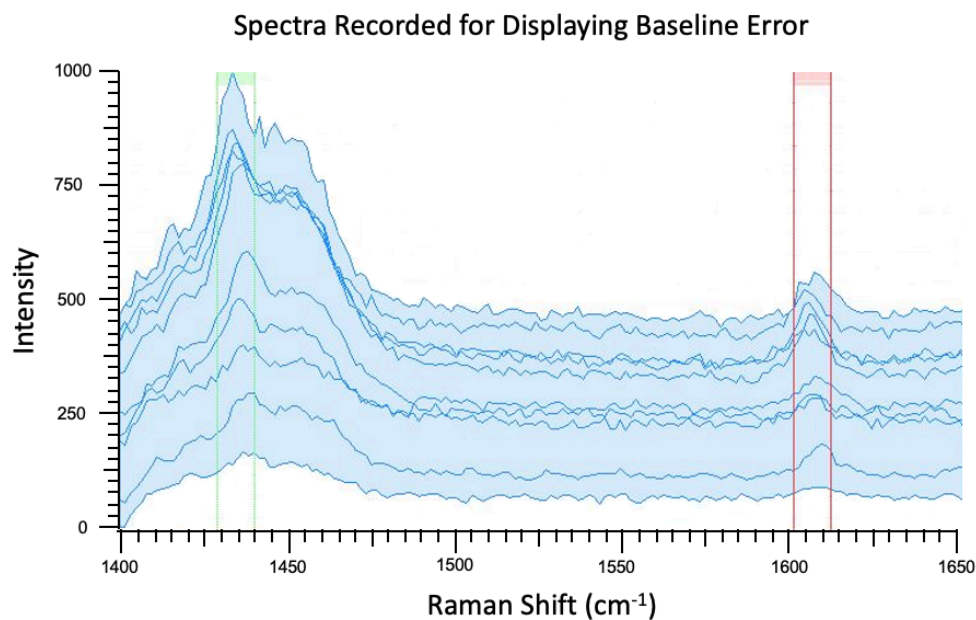


Figure 15. Composition of Spectra Displaying Baseline Error.

Another issue that was experienced was laser pulsing. With this issue, the intensity of the laser light would fluctuate. This was very apparent within the Raman maps as sections of the map would be significantly lower in intensity. Due to these Raman maps taking many hours to produce, large portions of the data would be unreliable. All of these issues became more relevant as the area mapped was increased significantly. In an effort to determine the size limit of the instrument, a $25,000,000\mu\text{m}^2$ area with a larger step size of $25\mu\text{m}$ was analyzed. This was performed with the 532nm Nd:YAG laser, 100% laser power, and the 600gr/mm grating with an acquisition time of 3 seconds for two acquisitions. The Spectra recorded and composite image are shown below in **Figure 16** and **Figure 17**.

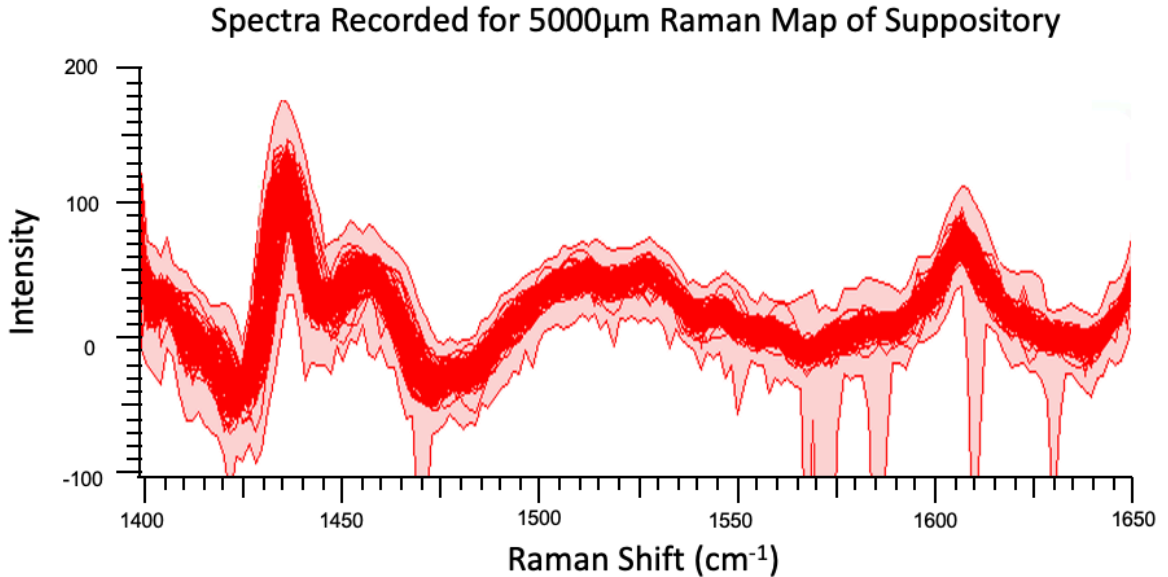


Figure 16. Composition of Spectra Gathered from $25,000,000\mu\text{m}^2$ area.

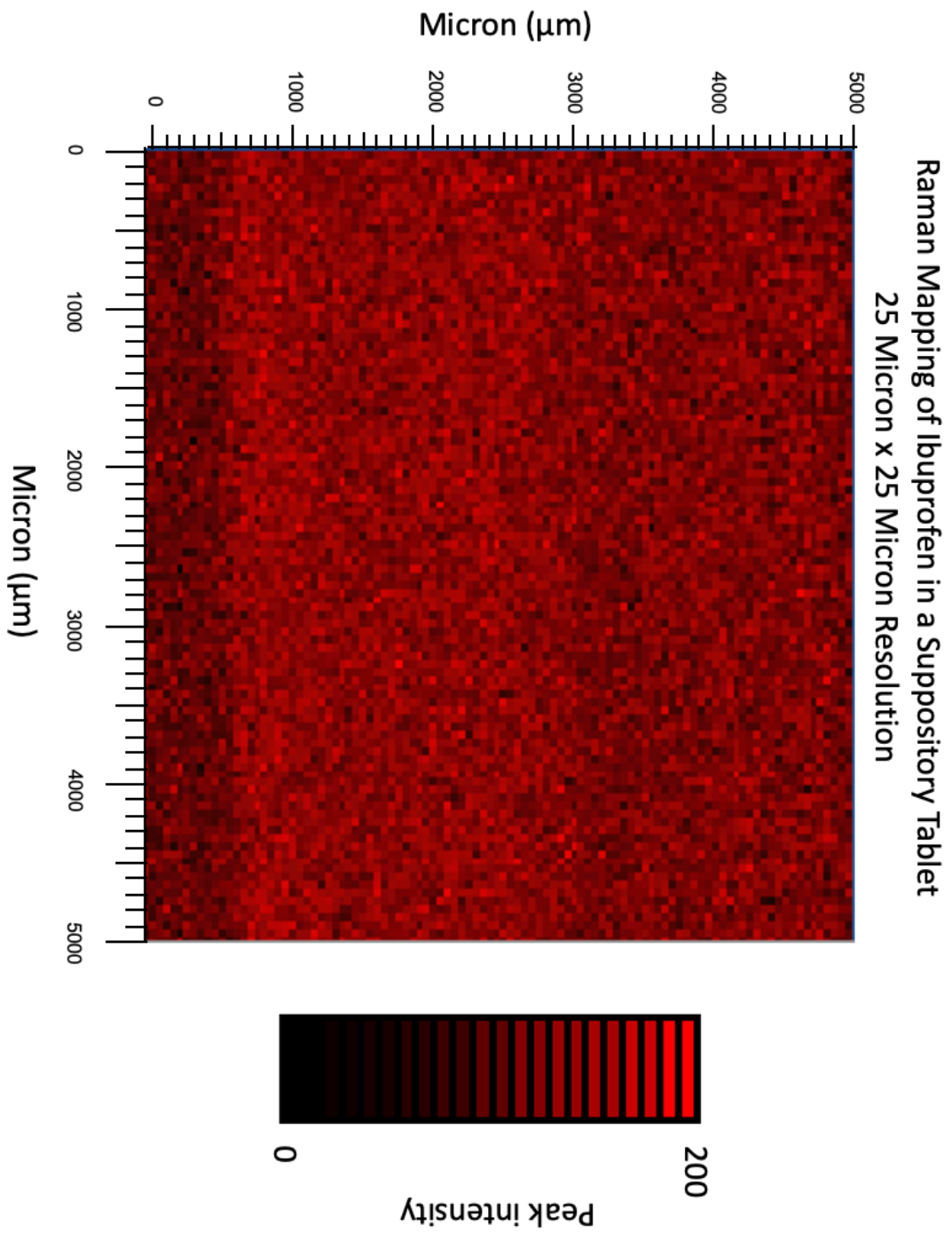


Figure 17. 25,000,000 μm^2 Raman Map of Ibuprofen with 25-micron Resolution.

Unlike the other Raman maps produced, no clear insights regarding the ibuprofen distribution are seen. It seems like a homogenous mixture, but that is not what was seen in the higher resolution maps. This indicates that most likely too large of a step size was used to accurately map ibuprofen within the sample. However, this Raman map was produced over the course of 67 hours. Therefore, a smaller steps size is not reasonable for research purposes as it would take even longer to produce the Raman maps. Furthermore, this 25,000,000 μm^2 area is still significantly smaller than the cross section of the suppository. In addition, due to the very long total acquisition time, dimming of the laser was seen toward the bottom of the map as can be seen in **Figure 17**.

Further data was set to be gathered, but, due to the COVID-19 outbreak, this was not feasible. However, it was still possible to produce conclusions from the gathered data to date.

Chapter 5: Conclusions and Future Work

Based on the data, it can be concluded that further research should be conducted over smaller areas with smaller step sizes. Larger sizes take significantly longer to produce and produce less accurate descriptions of the distribution of analytes. Furthermore, this analysis could be performed with more analytes, but would require a larger range of wavenumbers and analyte specific peaks that are easily visible when analyzed within the mixture. However, analysis on the overall distribution of ibuprofen throughout the suppository is not feasible with the current equipment due to the large sizes of the cross sections and acquisition times associated with this method. On the other hand, optimization and the limitations of the method were successfully discovered. Further uses of this method should be performed over smaller surface areas, or in a similar manner to the experiment probing the aggregation of α -synuclein amyloids, where spectra gathered with Raman mapping were averaged to acquire a more representative spectrum. To perform large area Raman maps, specialized equipment, such as the Renishaw inVia™ Qontor® which is specifically designed for rapid large area Raman imaging, should be used to better understand the overall distribution of analytes within the system.³⁷ However, a decently representative distribution could be achieved by combining data taken from different grid points as proposed by a previous experiment.²¹

References:

1. Pharmaceutical. <https://www.britannica.com/technology/pharmaceutical> (accessed 4/14).
2. Administration, F. D., A History of the FDA and Drug Regulation in the United States FDA centennial: 2006.
3. Step 1: Discovery and Development. <https://www.fda.gov/patients/drug-development-process/step-1-discovery-and-development> (accessed 4/14).
4. Step 2: Preclinical Research. <https://www.fda.gov/patients/drug-development-process/step-2-preclinical-research> (accessed 4/14).
5. Badyal, D. K.; Desai, C., Animal use in pharmacology education and research: the changing scenario. *Indian Journal of Pharmacology* **2014**, *46* (3), 257-65.
6. Step 3: Clinical Research. <https://www.fda.gov/patients/drug-development-process/step-3-clinical-research> (accessed 4/14).
7. Step 4: FDA Drug Review. <https://www.fda.gov/patients/drug-development-process/step-4-fda-drug-review> (accessed 4/14).
8. Step 5: FDA Post-Market Drug Safety Monitoring. <https://www.fda.gov/patients/drug-development-process/step-5-fda-post-market-drug-safety-monitoring>.
9. Bushra, R.; Aslam, N., An overview of clinical pharmacology of Ibuprofen. *Oman Medical Journal* **2010**, *25* (3), 155-1661.
10. Ricciotti, E.; FitzGerald, G. A., Prostaglandins and inflammation. *Arteriosclerosis, Thrombosis, and Vascular Biology* **2011**, *31* (5), 986-1000.
11. Evans, A. M., Comparative pharmacology of S(+)-ibuprofen and (RS)-ibuprofen. *Clinical Rheumatology* **2001**, *20 Suppl 1*, S9-14.
12. 5.2 Speed of Drug Effect. <https://www1.health.gov.au/internet/publications/publishing.nsf/Content/drugtreat-pubs-front6-wk-toc~drugtreat-pubs-front6-wk-secb~drugtreat-pubs-front6-wk-secb-5~drugtreat-pubs-front6-wk-secb-5-2>.
13. Baviskar, P.; Bedse, A.; Sadique, S.; Kunde, V.; Jaiswal, S., Drug delivery on rectal absorption: Suppositories. *International Journal of Pharmaceutical Sciences Review and Research* **2013**, *21*, 70-76.
14. Tro, N. J., *Chemistry : Structure and Properties*. p 1 volume (various pages).

15. Granger, R. M., *Intrumental Analysis: Revised Edition*. 1st ed.; Oxford University Press: United States of America, 2017.
16. The Raman Effect.
<http://www.acs.org/content/acs/en/education/whatischemistry/landmarks/ramaneffect.html> (accessed 4/18).
17. What are the most common applications of Raman spectroscopy?
<https://www.horiba.com/us/en/scientific/products/raman-spectroscopy/raman-academy/raman-faqs/what-are-the-most-common-applications-of-raman-spectroscopy/> (accessed 4/18).
18. Atkins, P. W., *Elements of Physical Chemistry*. 6th ed.; W. H. Freeman and Co.: New York, NY, 2013.
19. Gordon, K. C.; McGoverin, C. M., Raman Mapping of Pharmaceuticals. *International Journal of Pharmaceutics* **2011**, *417* (1), 151-162.
20. Zetterholm, S. G.; Verville, G. A.; Boutwell, L.; Boland, C.; Prather, J. C.; Bethea, J.; Cauley, J.; Warren, K. E.; Smith, S. A.; Magers, D. H.; Hammer, N. I., Noncovalent Interactions between Trimethylamine N-Oxide (TMAO), Urea, and Water. *The Journal of Physical Chemistry B* **2018**, *122* (38), 8805-8811.
21. Bell, S. E. J.; Beattie, J. R.; McGarvey, J. J.; Peters, K. L.; Sirimuthu, N. M. S.; Speers, S. J., Development of sampling methods for Raman analysis of solid dosage forms of therapeutic and illicit drugs. *Journal of Raman Spectroscopy* **2004**, *35* (5), 409-417.
22. Gowen, A. A.; O'Donnell, C. P.; Cullen, P. J.; Bell, S. E. J., Recent applications of Chemical Imaging to pharmaceutical process monitoring and quality control. *European Journal of Pharmaceutics and Biopharmaceutics* **2008**, *69* (1), 10-22.
23. Vajna, B.; Farkas, I.; Szabo, A.; Zsigmond, Z.; Marosi, G., Raman microscopic evaluation of technology dependent structural differences in tablets containing imipramine model drug. *Journal of Pharmaceutical and Biomedical Analysis* **2009**, *51*, 30-8.
24. Arruabarrena, J.; Coello, J.; MasPOCH, S., Raman spectroscopy as a complementary tool to assess the content uniformity of dosage units in break-scored warfarin tablets. *International Journal of Pharmaceutics* **2014**, *465* (1-2), 299-305.
25. Zhang, L.; Henson, M. J.; Sekulic, S. S., Multivariate data analysis for Raman imaging of a model pharmaceutical tablet. *Analytica Chimica Acta* **2005**, *545* (2), 262-278.

26. Rantanen, J., Process analytical applications of Raman spectroscopy. *The Journal of Pharmacy and Pharmacology* **2007**, *59* (2), 171-7.
27. Wang, H.; Barona, D.; Oladepo, S.; Williams, L.; Hoe, S.; Lechuga, D.; Vehring, R., Macro-Raman spectroscopy for bulk composition and homogeneity analysis of multi-component pharmaceutical powders. *Journal of Pharmaceutical and Biomedical Analysis* **2017**, *141*.
28. Eksi-Kocak, H.; Ilbasemis Tamer, S.; Yilmaz, S.; Eryilmaz, M.; Boyaci, I. H.; Tamer, U., Quantification and spatial distribution of salicylic acid in film tablets using FT-Raman mapping with multivariate curve resolution. *Asian Journal of Pharmaceutical Sciences* **2018**, *13* (2), 155-162.
29. Flynn, J. D.; Jiang, Z.; Lee, J. C., Segmental ¹³C-Labeling and Raman Microspectroscopy of α -Synuclein Amyloid Formation. *Angewandte Chemie International Edition* **2018**, *57* (52), 17069-17072.
30. Vajna, B.; Farkas, I.; Farkas, A.; Pataki, H.; Nagy, Z.; Madarász, J.; Marosi, G., Characterization of drug–cyclodextrin formulations using Raman mapping and multivariate curve resolution. *Journal of Pharmaceutical and Biomedical Analysis* **2011**, *56* (1), 38-44.
31. Čapková-Helešicová, T.; Pekárek, T.; Schöngut, M.; Matějka, P., New designed special cells for Raman mapping of the disintegration process of pharmaceutical tablets. *Journal of Pharmaceutical and Biomedical Analysis* **2019**, *168*, 113-123.
32. Matthaus, C.; Kale, A.; Chernenko, T.; Torchilin, V.; Diem, M., New ways of imaging uptake and intracellular fate of liposomal drug carrier systems inside individual cells, based on Raman microscopy. *Molecular Pharmaceutics* **2008**, *5* (2), 287-93.
33. Xu, Z.; He, Z.; Song, Y.; Fu, X.; Rommel, M.; Luo, X.; Hartmaier, A.; Zhang, J.; Fang, F., Topic Review: Application of Raman Spectroscopy Characterization in Micro/Nano-Machining. *Micromachines* **2018**, *9* (7).
34. Windbergs, M.; Haaser, M.; McGoverin, C. M.; Gordon, K. C.; Kleinebudde, P.; Strachan, C. J., Investigating the relationship between drug distribution in solid lipid matrices and dissolution behaviour using Raman spectroscopy and mapping. *Journal of Pharmaceutical Sciences* **2010**, *99* (3), 1464-75.
35. Raman Spectroscopy for Analysis and Monitoring In *RAMAN DATA AND ANALYSIS* Horiba.

36. Sakamoto, T.; Matsubara, T.; Sasakura, D.; Takada, Y.; Fujimaki, Y.; Aida, K.; Miura, T.; Terahara, T.; Higo, N.; Kawanishi, T.; Hiyama, Y., Chemical mapping of tulobuterol in transdermal tapes using microscopic laser Raman spectroscopy. *Die Pharmazie* **2009**, *64* (3), 166-71.
37. inVia™ Qontor® confocal Raman microscope.
<https://www.renishaw.com/en/invia-qontor-confocal-raman-microscope--38125>
(accessed 4/16).